LAPPEENRANTA UNIVERSITY OF TECHNOLOGY
Faculty of Technology
Master's Degree Program in Technomathematics and Technical Physics

Ivan Zotkin

# MODIFICATION OF A QUANTUM EFFICIENCY MEASUREMENT SYSTEM FOR MULTI-JUNCTION SOLAR CELLS

Examiners: Professor Erkki Lähderanta

Professor Mircea Guina

Supervisor: Ph.D. Antti Tukiainen

**ABSTRACT**
Lappeenranta University of Technology
Faculty of Technology
Master's Degree Program in Technomathematics and Technical Physics

Ivan Zotkin

**Modification of a quantum efficiency measurement system for multi-junction solar cells**

Master's thesis

2015

46 pages, 29 figures and 2 tables.

Examiners: Professor, Erkki Lähderanta
Professor, Mircea Guina

Keywords: solar cells, quantum efficiency, sensors, multi-junction solar cells, silicon, arsenide gallium

In this thesis the basic structure and operational principals of single- and multi-junction solar cells are considered and discussed. Main properties and characteristics of solar cells are briefly described.

Modified equipment for measuring the quantum efficiency for multi-junction solar cell is presented. Results of experimental research single- and multi-junction solar cells are described.

**PREFACE**

This work has been carried out at Optoelectronics Research Centre of Tampere University of Technology.

I wish to thank Professor Mircea Guina for giving me opportunity and support to write diploma at ORC laboratory.

I wish to express my gratitude to my supervisor PhD Antti Tukiainen for his support and guidance during experiments and writing my diploma work.

Big thanks and regards to Professor Erkki Lähderanta for his support during my studies at Lappeenranta University of Technology.

Associate Professor Svetlana Zubko has been very helpful with her scientific guidance and inspiring motivation, so I would like to declare that without Svetlana's help this work would not be possible.

Tampere, St.Petersburg 2012 – 2015
Ivan Zotkin

**TABLE OF CONTENTS**

**ABBREVIATIONS AND SYMBOLS** **5**

**1 INTRODUCTION** **7**

**2 BASIC PROPERTIES, OPERATIONAL CHARACTERISTICS OF SOLAR CELLS** **9**

2.1 Solar energy transformation into electricity: methods and features 9
2.2 Single-junction solar cells 16
2.3 Multi-junction solar cells 24
2.4 Internal and External Quantum efficiencies 32

**3 MOUNTING SYSTEM FOR QUANTUM EFFICIENCY MEASUREMENTS** **34**

3.1 Original system and measurement technique 34
3.2 Improvements made to the new system 36
3.2.1 Light bias 37
3.2.2 Covering against stray light 40

**4 EXPERIMENTAL RESULTS** **41**

**5 PERSPECTIVES AND CONCLUSIONS** **44**

**REFERENCES** **45**

## ABBREVIATIONS AND SYMBOLS

### Symbols

| | |
|---|---|
| $E_{ph}$ | Photon energy |
| $E_g$ | Band gap energy |
| $R$ | Spectral responsivity |
| $I_{ph}$ | Photocurrent |
| $I_s$ | Saturation current |
| $\lambda$ | Wavelength of photon |
| $h$ | Planck constant |
| $e$ | Elementary electric charge |
| $k$ | Boltzmann constant |
| $R_{Sh}$ | Shunt resistance |
| $R_S$ | Series resistance |
| $V$ | Voltage |
| $I_r$ | Radiation intensity |
| $S$ | Area of *p*–*n*-junction |
| $T$ | Temperature |
| β | Quantum yield |
| ν | Frequency |
| $I_{sc}$ | Short-circuit current |
| $V_{oc}$ | Open-circuit voltage |
| $P_{max}$ | Maximum power |
| $I_{max}$ | Maximum current |
| $V_{max}$ | Maximum voltage |
| $Q$ | Collecting efficiency |
| $Ø$ | Density of photon flux |

**Abbreviations**

| | |
|---|---|
| 1J | Single-junction |
| 2J | Double-junction |
| 3J | Three-junction |
| MJ | Multi-junction |
| TJ | Tunnel junction |
| QE | Quantum efficiency |
| IQE | Internal quantum efficiency |
| EQE | External quantum efficiency |
| PV | Photovoltaic |
| LED | Light Emitting Diode |
| IR | Infra-Red |
| FF | Fill Factor coefficient |
| MOCVD | Molecular Organic Chemical Vapour Deposition |
| MBE | Molecular Beam Epitaxy |

# 1 INTRODUCTION

Energy of the sun is the source of nearly all energy on the earth. In particular, wind energy that has been used hundreds of years to produce mechanical energy, uses air currents created by solar heated air and by the rotation of the earth. Even hydroelectricity is derived from the Sun (Honsberg Ch. et al. 2010). It is projected that global population and economic growth will more than double the energy consumption rate by the middle of this century, and photovoltaics is expected to make a considerable contribution to world electricity production. By the end of this century, the solar energy is predicted to become dominating part from the whole energy production up to 60%. Now price of electricity produced by photovoltaics is evaluated 20 – 60 eurocents per kilowatt-hour; compared to the price of electricity from traditional power supplies 2 – 3 eurocents per kilowatt-hour.

Currently the production of photovoltaic energy is constantly increasing due to different reasons: this power generation is reliable, it does not have any moving parts and care costs are quite cheap. Other positive advantages are the following: photovoltaic system is silent, and it has no effect on the atmosphere (Markvart, T. 1994). In other words, it is “green” energy that brings no pollution to the atmosphere. A solar cell is an electronic device which converts sunlight into electricity due to the photoeffect in a semiconductor. Nowadays research of solar cells is considered as one of the interesting areas from the side of manufacturing relatively cheap semiconductor devices for electricity generation using solar flux.

Presently solar cells are used in a quite huge amount of terrestrial applications in locations where other ways of electricity production and delivery are not possible at all. From the other side, solar cells production and installation have quite high capital costs compared with the amount of electricity they produce. It is described by a quantum efficiency parameter. This parameter is determined by the ratio of the carriers collected from the solar cell to the photon amount that got into a cell.

Solar cells studies in our days cover different materials and different structures to achieve maximum power from the cell trying to keep the cost to a minimum. One stimulating

aspect of multi-junction solar cells is that there are still a lot of opportunities to explore. In comparison with the achieved efficiencies of single-junction solar cells that have almost reached their potential limits, multi-junctions photovoltaics have still room for maneuver: a current record of efficiency is 46% with the theoretical limit of 86.8%.

Photovoltaic industry is growing considerably each year, and high-efficiency multi-junction solar cells will help the solar industry to develop even faster.

A lot of experiments and measurements have been done for the one *p*–*n*-junction solar cells, called single junction (1J) solar cells. In order to increase the conversion efficiency and cover wider wavelength range, double junctions (2J) and triple junctions (3J) solar cells have been produced. For multi-junction cells it is important to be able to characterize the sub-junctions of 2J and 3J cells. This can be done by measuring the quantum efficiencies of the sub-junction separately. So far, the university laboratory had the equipment only for characterization of 1J solar cells quantum efficiency, but not for measuring 2J or 3J cells.

The present master's thesis is dedicated to the system modification for measuring one of the main characteristics of solar cells – quantum efficiency. The thesis describes research and manufacturing of solar cells justified by present electricity demands, types of photovoltaics, existing and modified measurements systems, and scientific results of wavelength dependence of quantum efficiency for the single- and multi-junction solar cell produced in ORC laboratory.

# 2 BASIC PROPERTIES, OPERATION PARAMETERS OF SOLAR CELLS

## 2.1 Solar energy transformation into electricity: methods and features

Generally, it is possible to divide all detectors into two separate groups: thermal and quantum detectors. Quantum detectors relate to the absorption of radiant energy quantum, that is an evaluation of the quanta ration interacted with the detector. For thermal detectors, the radiation heats the detector element, and the consequent temperature is measured (Young M., 1977). Solar cell is a quantum detector.

Basically, a solar cell is an electrical device that transforms solar energy into electricity due to an *internal photoelectric effect*, which is the excitation of an electron by a quantum of light radiation. The quantum energy, however, is not sufficient to free the electron from the detector surface and is enough to change the electrical properties of the material. In other words, the basic process of electrons redistribution in energy states under light radiation influence that take place inside the semiconductors is called an internal photoeffect. The term *photovoltaic effect* describes the generation of voltage or electric current in a semiconductor under exposure to light radiation. These effects are directly related to each other but they are different processes.

Photons incident on the surface of a semiconductor will be either reflected from the top surface, or will be absorbed in the material, or, failing both above processes, will be transmitted through the material. The absorbed photon has the possibility of exciting an electron from the valence band to the conduction band. A key factor in determining whether a photon is absorbed or transmitted is the ratio of the photon energy to the forbidden band of semiconductor. Therefore, only if the photon has enough energy the electron will be excited into the conduction band from the valence band.

Fig. 1 illustrates three cases describing interaction of the incident photons with semiconductor material depending on the ratio of the photon energy $E_{ph}$ and semiconductor band gap $E_g$:

1. $E_{ph} < E_g$: photons with energy $E_{ph}$ less than the band gap $E_g$ weakly interact with the semiconductor, passing through it as if it is transparent (Fig. 1 a).

2. $E_{ph} > E_g$: photons with the energy greater than the band gap are strongly absorbed. This case is shown in Fig. 1 b. In this case a photon produces an electron-hole pair.
3. $E_{ph} = E_g$: photons have just enough energy to create an electron-hole pair and are efficiently absorbed in semiconductor (Fig 1 c). In this case the energy transfer is as close to 100% efficient as is thermodynamically possible.

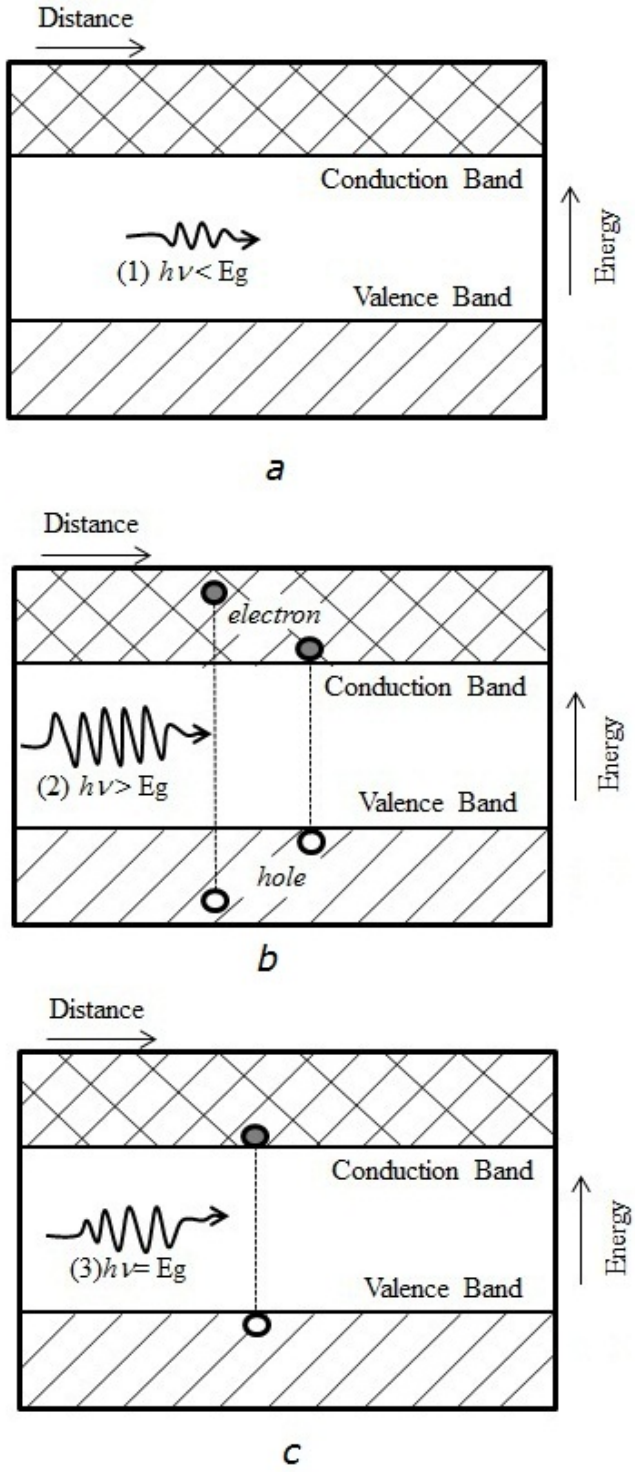


Fig. 1. Energy diagrams of semiconductor describing cases: (a) $E_{ph} < E_g$, (b) $E_{ph} > E_g$, (c) $E_{ph} = E_g$.

In other words, operational energy range of a solar cell is defined by photon energies that are equal or higher than the semiconductor band gap. These cases are shown in Fig 1 *b* and *c*.

Solar cells can be classified by materials that they are made of (see Fig. 2). Wide spectrum of solar cells is produced from semiconductors: typical semiconductors like Ge and Si, semiconductor compound $A^{III}$ $B^{V}$ and compounds $A^{II}$ $B^{VI}$. The first generation of solar cells was made from the crystalline silicon. The second generation cells were thin-film solar cells including amorphous silicon and chemical compounds based on CdS, CdTe (Afanasev, V. et al. 2011).

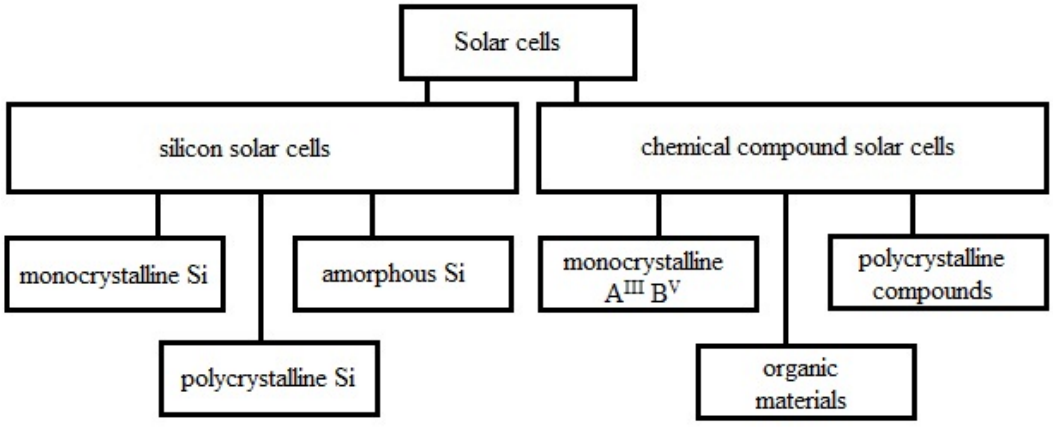


Fig. 2. Classification of solar cells by materials and materials structure.

Silicon, which is an element from the group IV, is the most commonly used semiconductor material, as it forms the basis for integrated circuit chips. The most mature technology and most solar cells are also silicon based. Laboratory efficiency of monocrystalline silicon solar cells is about 25%, of multicrystalline ones it is about 20% , and of amorphous silicon solar cells is about 13% (Philipps, S. et al. 2014). Some other semiconductors used for producing solar cells are AlP, GaP, InP, GaAs. Using of these materials and their compositions makes it possible to achieve required width of a bandgap determining the operational wavelength range.

The main restrictions of silicon solar cells are surface reflection of incident radiation, recombination and parasitic resistances. These factors result in decreasing of a solar cell efficiency. The value of the theoretical efficiency is about 25%.

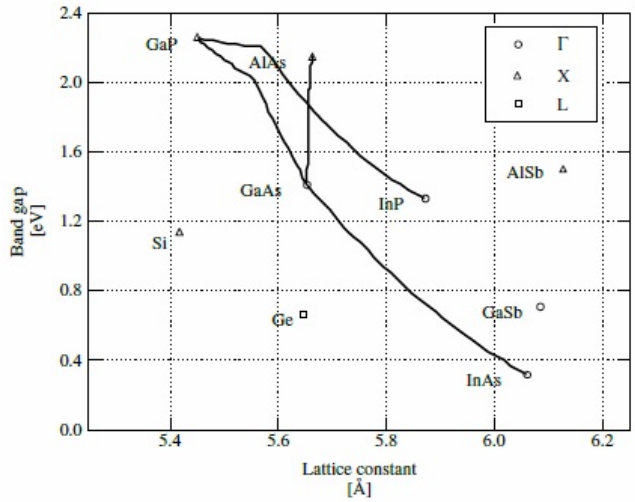


Fig. 3. Estimated bandgaps as a function of lattice constant for Si, Ge, III-V binaries and their alloys (Luque et.al. 2011).

Fig. 3 represents the dependence of bandgaps on lattice constants for some materials from IV and III-V groups. As one can see, it is possible to choose a proportion of alloy components in a way that a bottom cell material has a lattice-matched interconnecting tunnel-junction and has less defects that produce the lattice mismatching of top and bottom cells. It was presented that for tandem cells it is possible to produce such lattice matching with a theoretical efficiency of about 36% (Luque et.al. 2011).

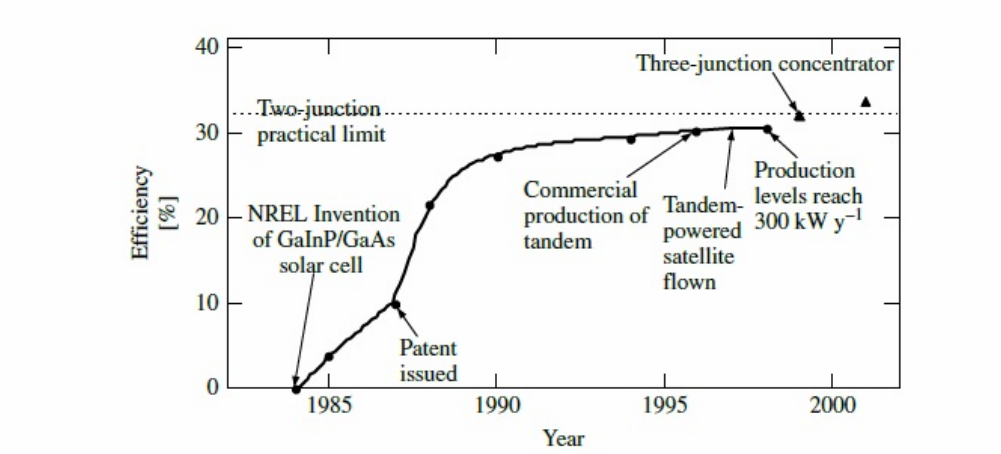


Fig. 4. Time diagram showing the progress in two-junction GaInP/GaAs solar cells efficiencies. These efficiencies have been measured at AM1.5 global spectrum.The triangles show samples measured under concentrated sunlight for three-junction GaInP/GaAs/Ge cells (Luque et.al. 2011).

A fifteen-year progress in increasing of two-junction GaInP/GaAs solar cell efficiency is shown in Fig. 4. It demonstrates the 33% practical limit of efficiency.

The National Renewable Energy Laboratory (NREL) has compiled all the data about the highest confirmed conversion efficiencies for the solar cells types from 1976 to the present. Recent achievements in the increasing of the multi-junction solar cell conversion efficiencies are illustrated in Fig. 5. Cell efficiency results are provided within different families of semiconductors: (1) multi-junction cells, (2) single-junction gallium arsenide cells, (3) crystalline silicon cells, (4) thinfilm technologies, and (5) emerging photovoltaics. The plot is courtesy of the National Renewable Energy Laboratory, Golden, CO.

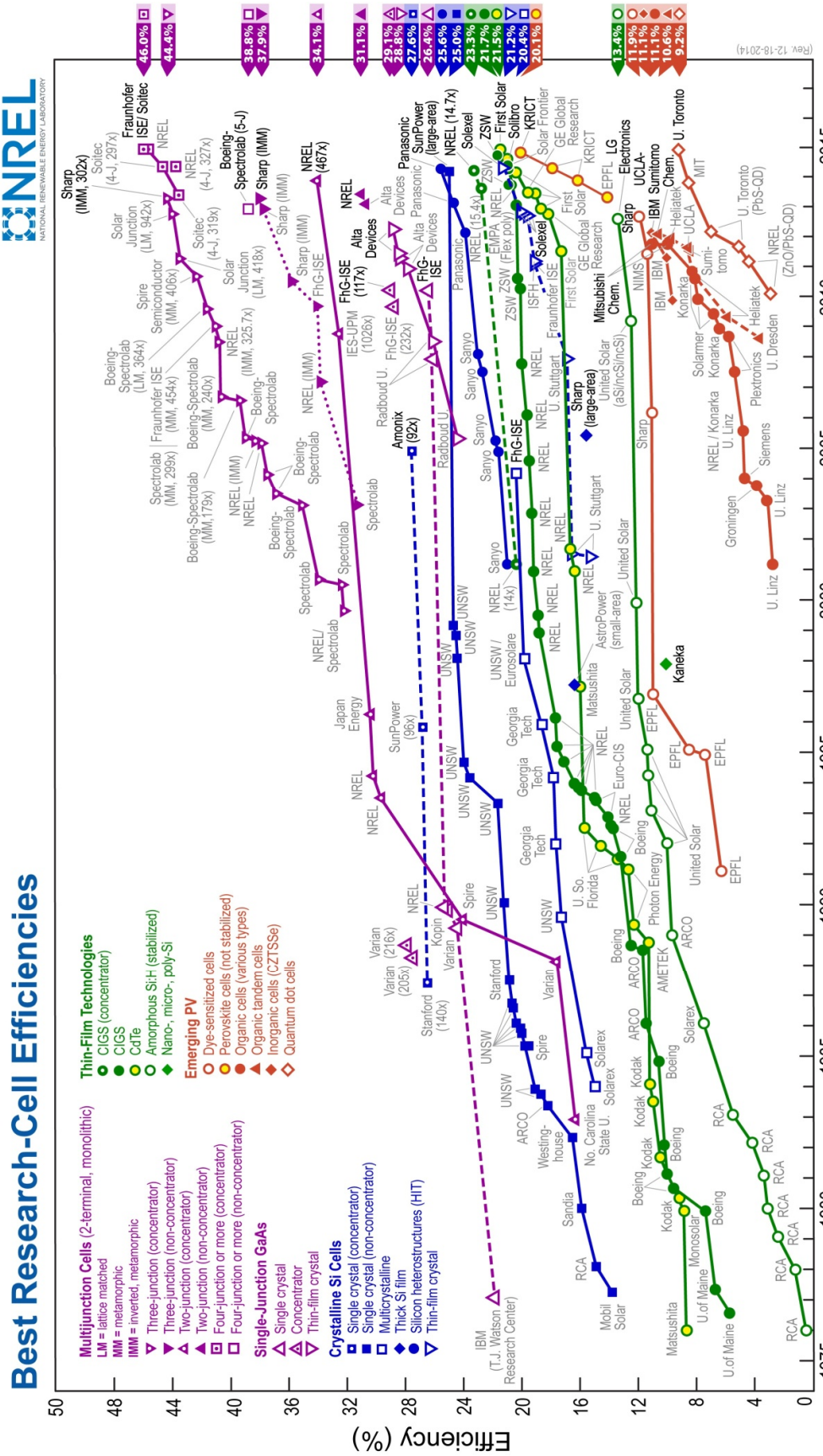


Fig.5. Reported timeline of solar cell energy conversion efficiencies. This plot is courtesy of the National Renewable Energy Laboratory, Golden, CO (NREL, 2015).

## 2.2. Single-junction solar cell

The simplest solar cell consists of two semiconductor layers with different types of conductivity. Such solar cell is called single junction (1J) solar cell. A typical single solar cell structure is shown in Fig. 6.

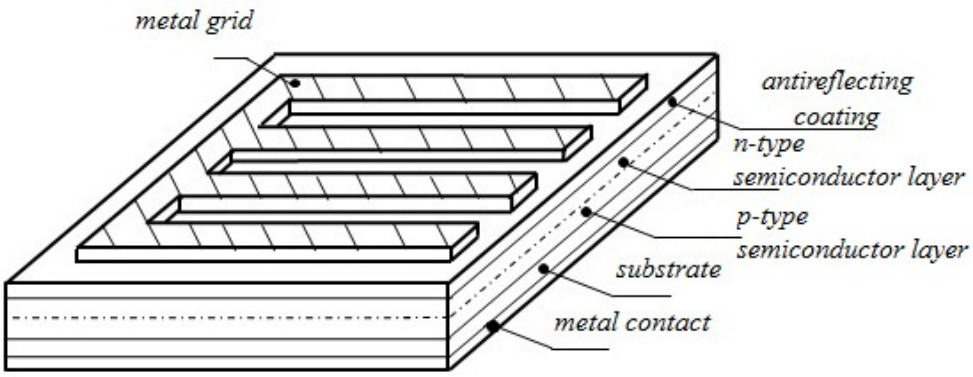


Fig. 6. A single junction solar cell schematic view.

A solar cell consists of a substrate with the bottom conducting electrode, two semiconducting layers forming a *p*–*n*-junction and top anti-reflecting coating. This coating is supposed to reduce the reflection of light radiation from the cell surface. A metal grid placed on the top of the cell is the second conducting electrode which helps to collect carrier charges produced by the internal photoelectric effect. Obviously, the grid reduces the working surface of the cell decreasing the amount of photons penetrating into the solar cell. It is necessary to choose the optimal shape of grid to increase the amount of photons passed through the cell.

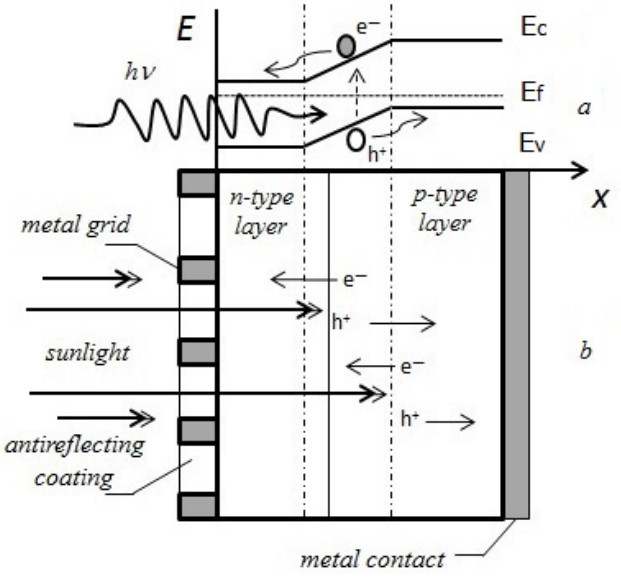


Fig. 7. *a.* basic principle of internal photoeffect showing on a bandgap of a *p-n* junction, *b.* a schematic view of single junction solar cell interacting with a sunlight radiation.

Schematic illustration of the internal photoeffect in a *p–n*-junction is shown in Fig. 7. A photon with the energy that is higher than the width of the junction bandgap produces an electron-hole pair (Fig. 7. *a*). Cross section of solar cell and interaction of sunlight with semiconductor layers is represented in Fig. 7. *b*. During irradiating the junction, electrons from valence band are excited to the conduction band, creating electron-hole pairs. Due to the strong electric field in the junction area, the charge carriers are enforced to move in opposite directions restricting the process of recombination. Near the *p–n*-junction the depletion layer is formed by the migration of mobile charge carriers between *p*- and *n*-type semiconductor layers. Electron-hole pairs in depletion region are restrained from recombination by the presence of the built-in electric field, which sweep them apart (Bishop, R. 2002). Charge carriers generated in or near this area affect the amount of the photocurrent produced by the cell. Electron-hole pairs created deep in semiconductor must go through it before reaching the depletion region (Schroder, D. 2006). Out from the depletion region the charge carriers have more chances to get recombined. This possibility is evaluated by the term of diffusion length. That is the distance between the location of the charge carriers generation and the depletion region. It is an average pathway for electron or hole within the area outside the depletion region without an electrical field before recombination may occur (Kaltschmitt, M. et. al. 2007). Hence, the

charge carriers produced far from the depletion area doubtfully influence amount of the photocurrent since they have less probability to recombine with carriers of the other type.

Therefore, it is necessary to design the cell in a way that the optical absorption and the width of the depletion layer allow generating the maximum amount of the charge carriers in the depletion area.

The equivalent scheme of single junction solar cell is presented in Fig. 8. Basically, a solar cell can be pictured as a current generator connected in parallel with a diode. Taking into account the solar cell imperfection, the shunt resistance $R_{Sh}$ and the series resistance $R_S$ should be included. This model with a diode is one of the simple way to represent solar cell functioning. Also there more sophisticated small-signal models for semiconductor solar cells exist.

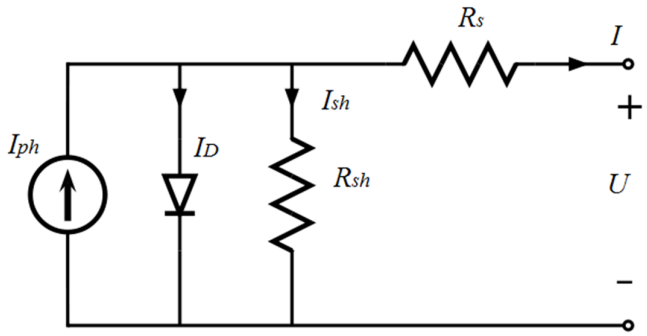


Fig. 8. Equivalent circuit of 1J solar cell (Lorenzo, E. et al. 1994).

A series resistance can be considered as a sum effect of substrate resistance; contact resistances of the top and bottom contacts; ohmic losses in the solar cell layers; ohmic losses at the heterojunction interfaces and ohmic losses in the metals (contact grid and bottom metal). The shunt resistance mainly is determined by the leakage current of *p*–*n*-junction.

On Fig. 9 two dependeces of current density from voltage for the such equivalent circuit are presented. One of the curve represents a dependece for ideal current density assuming shunt resistance equals zero. Another graph is the same dependance with the shunt resistance equals 100 ohm. This case has a certain curve slope near the short-circuit point. It is possible to determine approximately the shunt resistance value from this slope.

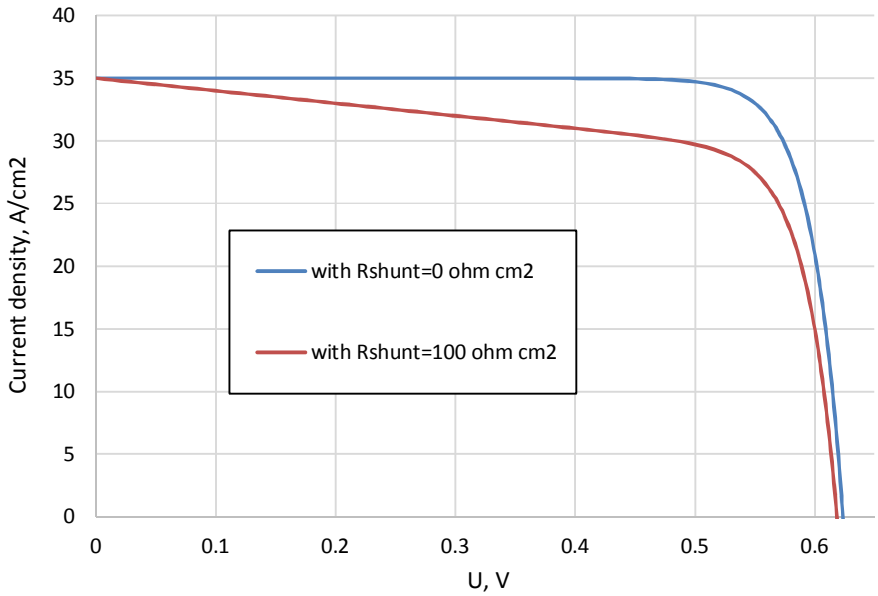


Fig. 9. Current density from voltage dependences with shunt resistance and for $R_{shunt}$=100 ohm. Curve data from (Honsberg, Ch. et al. 2010).

Presense of the series resestance gives effect on a curve slope near the open-cicrcuit point.

The amount of current produced by a solar cell is precisely related to the number of photons absorbed. The lower the bandgap, the more photons are absorbed and the greater is the number of electrons excited into the conduction band and free for current production (Burnett, B. 2002). The photon absorption does not happen exactly at the surface of semiconductor, but photons may go through deeply before being absorbed. For example, silicon and germanium have a much lower absorption coefficient than gallium arsenide at wavelengths close to their band gaps. Therefore, the thicker are the layers of silicon and germanium, the larger are the numbers of the absorbed energetic photons. Hence, generated current depends on the material thickness, its absorptivity and the ability to collect generated carriers. This ability depends on the diffusion length that correspondingly related to a semiconductor material doping. The higher is level of semiconductor doping, the lower is the diffusion length. (Kaltschmitt, K. et. al. 2007).

Current-voltage characteristic of a solar cell is described as follows:

$$I = I_s(e^{e\,V/k\,T} - 1) - I_{ph}, \qquad (1)$$

where $I_S$ is the saturation current and $V$ is the voltage over the cell. In equation (1) $I_s$ is a saturation current, $I_{ph}$ is a photocurrent that is amount of the excess charger carriers that have achieved a *p*–*n*-junction:

$$I_{ph} = \frac{e\,\gamma\beta I_r}{h\,\upsilon}. \qquad (2)$$

In the equations (1, 2) $e$ is elementary charge, $\gamma$ is an amount of unrecombined charge carrier pairs, $\beta$ is a quantum yield, $I_r$ is a radiation intensity, $k$ is Boltzmann constant, $T$ is a temperature, $h$ is Planck constant, $\upsilon$ is a frequency.

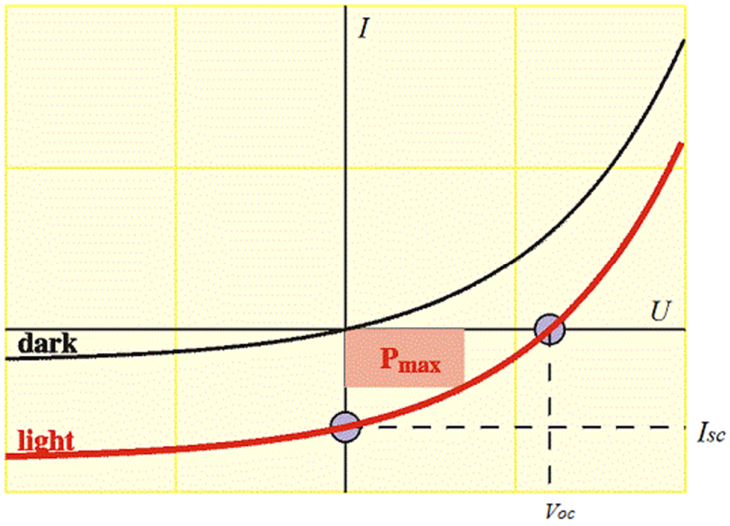


Fig. 10. *I-V* characteristic of a solar cell under light compared to a dark diode (Stallinga, P. 2009).

Typical shapes of *I-V* graphs for a diode in dark and for a solar cell under illumination are presented in a Fig. 10. The graphs illustrate the characteristics of solar cells: the short-circuit current $I_{sc}$, the open-circuit voltage $V_{oc}$, and the fill factor (FF) coefficient describing the maximum power $P_{max}$ produced by the cell. The output voltage of a photovoltaic cell is directly related to the energy of the electrons excited into the conduction band. The higher the bandgap, the greater the energy of the electrons in the conduction band must be. At zero cell voltage, the cell current equals to the short-circuit current: it is following from (1) that $I_{sc} = -I_{ph}$. From the other side, if the applied voltage becomes high enough so that recombination current is big as well, the solar cell current

reduces dramatically. The voltage at $I = 0$ corresponds to the open-circuit voltage $V_{oc}$ (Luque, A. & Hegedus, S. 2011). Assuming $I = 0$ in (1) the open-circuit voltage can be defined as

$$Voc = \frac{k\,T}{e} ln\left[\frac{I_{ph}}{I_s} + 1\right] = \frac{kT}{e} ln\left[\frac{e\,\beta\,\gamma\,S\,I_r}{h\,\upsilon\,I_s}\right]. \quad (3)$$

In (3) $S$ is the area of $p$–$n$-junction.

A solar cell does not produce any power under short or open circuit. The maximum power $P_{max}$ produced by the cell is shown in Fig. 11 and is described as following:

$$P_{max} = V_{max}\,I_{max} = \mathrm{FF}\;V_{oc}\,I_{sc}, \quad (4)$$

where $V_{max}$ and $I_{max}$ are the voltage and current at the maximum power point $P_{max}$. Here FF is a fill factor coefficient which is described in eq. (8). The $I_{max}$ is the current produced under maximum power conditions and is more representative than $I_{sc}$ for description of the operational performance. The maximum current $I_{max}$ can be found from the solution to the following equation

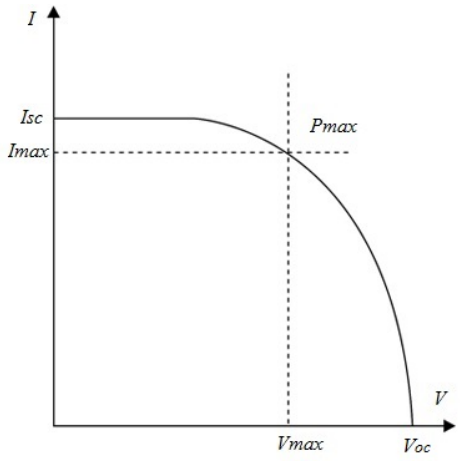


Fig. 11. *I-V* curve of a solar cell showing the maximum power point.

$$\frac{dP}{dV} = 0. \quad (5)$$

The maximum voltage can be derived from the solution to following equation

$$V_{max} \cong V_{OC} - \frac{k\,T}{e} ln\left[1 + \frac{e\,V_{max}}{k\,T}\right]. \quad (6)$$

The maximum current is

$$I_{max} = \frac{e\,I_s\,V_{max}}{k\,T} \exp[e\,V_{max}/(k\,T)] \approx I_{ph}\left(1 - \frac{k\,T}{e\,V_{max}}\right). \quad (7)$$

One of the most important performance parameters characterising the quality of a solar cell is a fill factor or a filling coefficient, which can be calculated as

$$\text{FF} = \frac{V_{max}\,I_{max}}{V_{oc}\,I_{sc}}. \quad (8)$$

A filling factor shows a difference between *I-V* curves of the real and ideal solar cells. In other words, this ration describes how the *I-V* curve of a real solar cell comes close to a perfect rectangle, which represents the ideal solar cell (Yastrebova N.V., 2007). FF for high-efficiently cells is typically in the range of 80% to 90%, where 100% would be ideal. Evidently, series and shunt resistances affect a form factor FF and an open-circuit voltage $V_{os}$.

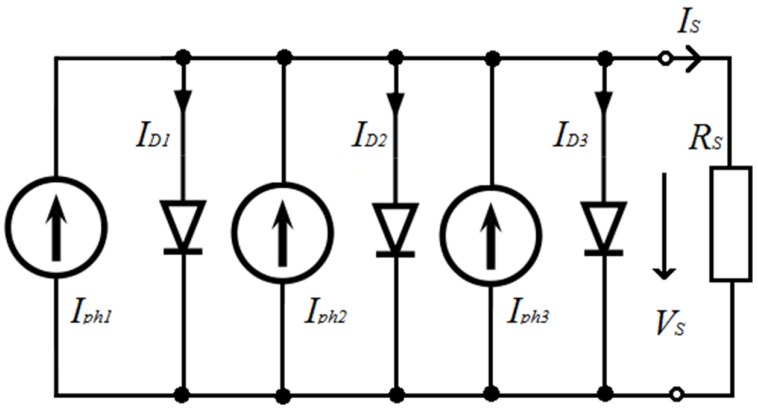


Fig. 12. Principal scheme of parallel-connected solar cells: $I_{ph}$ is a photocurrent, $I_D$ is a current through the diode.

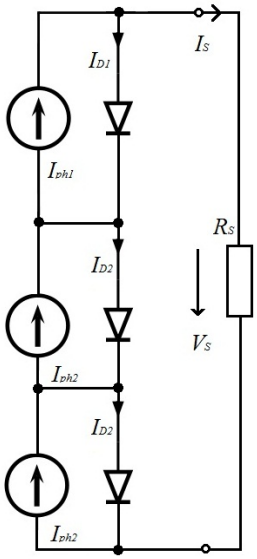


Fig. 13. Principal scheme of series-connected solar cells: $I_{ph}$ is a photocurrent, $I_D$ is a current through the diode.

The typical single solar cells have small values of the short-circuit current $I_{sc}$ and the open-circuit voltage $V_{oc}$, and therefore the small value of $P_{max}$. To achieve high values of the current, parallel connecting of photovoltaic cells is used (Fig. 12). To obtain high values of voltage, solar cells are connected in series. The series connection of solar cells is shown in Fig. 13. Volt-ampere characteristics of a single solar cell, parallel connection of solar cells, and series connection of solar cells are shown in Fig. 14. In the Fig. 14 circles represent the maximum power points (MPP).

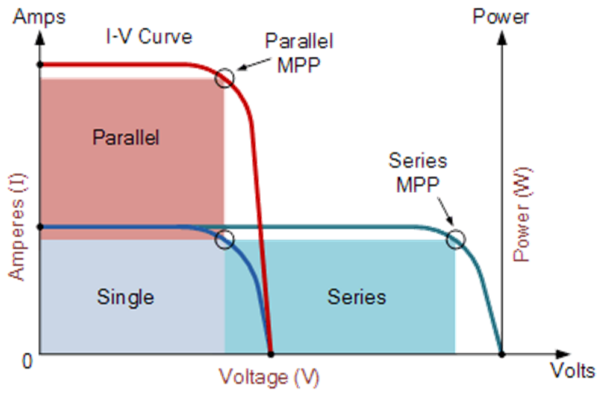


Fig. 14. *I-V* curves with corresponded maximum power points for the series- and parallel-connected solar cells.

It is important to take into account the power losses in solar cells. The fundamental loss is the transformation of energy into solar cell material heating. Some photons of solar spectrum have energy below the semiconductor bandgap. Such photons do not contribute into electricity generation and they are not absorbed by the semiconductor. In order to exclude such type of loss, tandem cells are used. The tandem cell is a stack of several cells made from different semiconductors. The top cell of the tandem cell is made of high-bandgap semiconductor converting the short-wavelength radiation. The light transmitted through the top cell is then converted by the bottom cell. Such structure allows increasing the achievable efficiency dramatically, and it will be discussed in the next section.

Another type of loss occurring in semiconductors is a process of recombination when an electron-hole pair is annihilated. This process occurs mainly in semiconductors with the high amount of impurities or defects in the crystal structure. Besides, electrons can move into the valence band and recombine with the holes at the surface of the semiconductor and at ohmic contacts. Possible way to decrease recombination processes is improving manufacturing technique of a semiconductor. During the cell manufacturing, the semiconductor surface is passivated with an oxide to reduce the surface recombination. The process of recombination affects both the voltage and current outputs (Markvart, T. 1994). Recombination leads to output current decreasing.

Light reflection from the top surface, cell shading by the top electrodes, and an incomplete absorption of light are other sources of loss in the solar cells. The incomplete absorption of light, especially in the crystalline silicon cells, has the biggest effect due to poor light absorption properties of silicon. Some manufactures place both contacting electrodes on the bottom of the cell to exclude the influence of shading from the top electrodes. There are several ways to decrease light reflection from the top surface: covering the cell with anti-reflecting coating, using surface texturing and making the bottom electrode optically reflecting to trap light inside of a sub-cell. Mixing these methods produces effective light trapping that allows thin silicon cells manufacturing (Markvart, T. 1994).

Different types of energy losses in solar cells with their corresponded contributions are represented in Table 1.

**Table 1**. Energy losses occurring in the semiconductor solar cells (Afanasiev, V. et al. 2011).

| **Type of energy loss** | **Amount of effect, %** |
|---|---|
| Photons with $h\nu < E_g$ | ~20 |
| Termalization | ~30 |
| Recombination losses in *p-n*-junction | ~20 |
| Incomplete collecting of photogenerated charge carriers | ~4 |
| Loss on shunt and series resistances | ~4 |
| Light reflection loss | ~2 |
| Top grid shading | ~4 |
| Non-photoactive losses | ~1 |

The main goal of solar cells design is maximizing the total generated power. Multi-junction photovoltaics, if compared to single-junction cells, have small currents because the total amount of photons is distributed over the several sub-cell layers. In this case, the photon amount available for electron exciting in one layer is decreased. At the same time, the excited electrons are more energetic and have a greater electric potential, so the reduction of currents is compensated by increasing in voltage. Thus, the overall power of the cell becomes higher. Additionally, the design of multi-junction cells is more beneficial, because the resistive losses, being proportional to the square of the current value, can be dramatically reduced (Yastrebova N.V., 2007).

The actual difference between the quantum efficiency (QE) and the energy conversion efficiency is that QE is a term inherent to the light absorbing material and cannot describe the cell in a whole. It refers to the ratio of the absorbed photons that produce electron-hole pairs. The energy conversion efficiency is the percentage of incident electromagnetic radiation that is converted to electrical power when a solar cell is connected to an electrical circuit. This efficiency actually depends on many factors, including the temperature, amount of incident radiation and the solar cell surface area.

In photovoltaics electron-hole pairs can be generated by solar radiation in *n*- and *p*-areas of the semiconductor depending on the depth where the photons with certain energy have been absorbed. The electric field collects electrons in *n*-area and holes in *p*-area. However, part of minority charge carriers can be lost due to recombination process. The collecting efficiency of photogenerated charge carriers is evaluated as a coefficient of collecting charge carriers $Q$. It is equal to the ratio of an electron-hole pair amount separated by *p*–*n*-junction to the whole amount of photogenerated electron-hole pairs:

$$Q = \frac{j_{ph}}{q \cdot \emptyset} \qquad (9),$$

where $j_{ph}$ is photocurrent density and $\emptyset$ is the density of photon flux falling on the cell surface.

## 2.3 Multi-junction cells

The Sun emits more photons in ultraviolet, visible and surrounding ranges, than in other parts of the spectrum. The red line in Fig. 15 represents the solar spectrum in the open space. The green line shows the solar spectrum near the Earth surface taking into account the photons absorbed by the atmospheric gases.

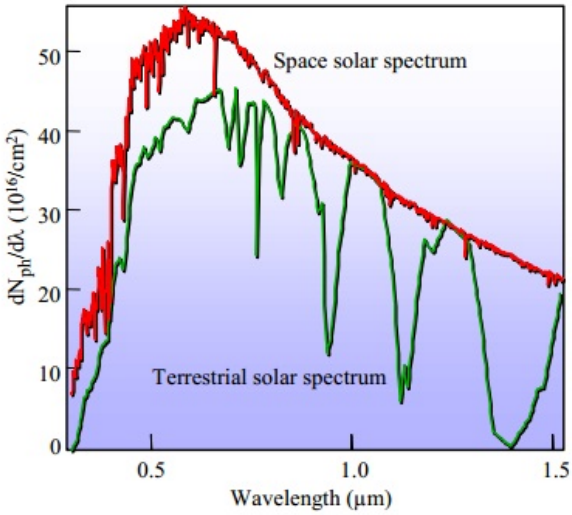


Fig. 15. Space and terrestrial solar spectrums (Yastrebova N.V., 2007).

Photovoltaics cells are created to trap the photons of the solar spectrum. The most important range from the sense of energy is the visible spectrum, but it is still a good idea to capture photons from near-infrared and ultraviolet spectrum as well. It has been advised to create several cells connected in series that are sensitive to a certain wavelength range to cover and collect maximum available photons. Semiconductor materials for a solar cell manufacturing are selected according to their bandgaps: photons with energies equal to or greater than the bandgap excite electrons into the conduction band (Burnett, B. 2002).

Values of 1J solar cell efficiency are quite low. The Shockley-Queisser limit describes the maximum theoretical efficiency of a solar cell. The calculated value of the solar conversion efficiency was around 33.7% for a single *p*–*n*-junction with a bandgap of 1.1 eV (Shockley, W. & Queisser, H. 1961). This efficiency limit can be exceeded using several junctions connected in series, in other words, multi-junction cells (MJ) with

stacked-configuration. Present theoretical researches demonstrated that the maximum conversion efficiency for ideal 1J solar cell is about 48% (Fig. 16).

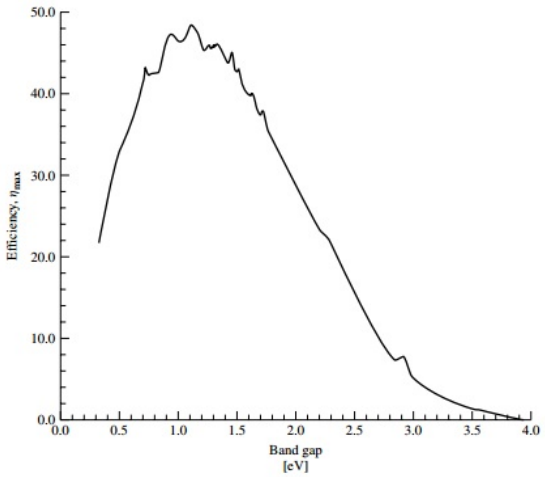


Fig. 16. Theoretical maximum efficiency as a function of semiconductor band gap for an AM 1.5 global spectrum (Luque, A. & Hegedus, S. 2011).

MJ solar cells can exceed the theoretical efficiency limit of 1J cell because of the ability to decrease the loss affected by interaction of the photons with energies higher than band gap with semiconductor crystal lattice.

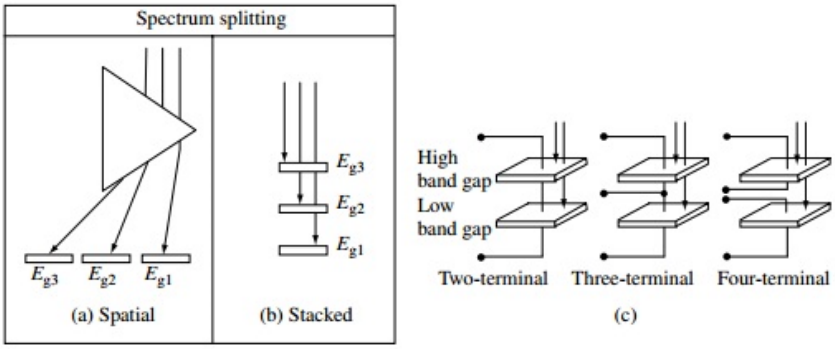


Fig. 17. Schematic comparison of (a) spatial-configuration approaches and (b) stacked-configuration approaches in distributing light to sub-cells with different bandgaps. (c) Illustration of two-, three-, and four-terminal connections of 2J cells (Luque, A. & Hegedus, S. 2011).

For the high-efficient solar cell producing, one has to use different materials with different bandgaps to cover more solar spectrum areas. One of the approaches is based on using an optically dispersive element such as a prism to spatially distribute the photons with

different energies to different locations, where the certain cells would be disposed to collect related photons (Fig. 17 (*a*)).

MJ solar cells can be manufactured either by mechanical stacking of independently grown layers, or each semiconductor layer can be monolithically grown on the top of another as one single piece. It could be done by the molecular organic chemical vapour deposition (MOCVD) or the molecular beam epitaxy (MBE) (Yastrebova N.V., 2007). For solar cell production, MOCVD has been and is still the most used technique, but MBE can be also used for volume production of multi-junction cells.

A generally preferable design of MJ cell is to put 1J cells stacked upon each other as illustrated in Fig. 17 (*b*). The top cell has a larger bandgap ($E_{g3}$) than the middle cell ($E_{g2}$). Such sub-cells disposition allows using the fact that junctions act as low-pass photon energy filters, transmitting only the sub-band gap light. In other words, as illustrated in Fig. 17 (*b*), photons with $hv > E_{g3}$ are absorbed by that junction, photons with $E_{g2} < hv < E_{g3}$ get absorbed by the junction with $E_{g2}$ bandgap and photons with $E_{g1} < hv < E_{g2}$ get absorbed by the junction with $E_{g1}$ bandgap. Such stacked configuration requires that all the junctions in the stack except the bottom one, be transparent to photons with the energy below sub-cells bandgaps. It can be quite challenging to choose the material of substrate and bottom electrode. One efficient way to solve the problem is to manufacture all the junctions, each one on a top of a previous one, monolithically on a single substrate, as it shown in Fig. 18. The figure represents a schematic cross-section of a monolithic two-terminal series-connected 3J solar cell.

Fig. 17 (*c*) illustrates three ways of sub-cells connection. Four-terminal configuration is the most convenient to use, since each sub-cell is electrically isolated from the other sub-cells and does not have restrictions on the sub-cell polarities and currents. However, this configuration has a processing issue after growth. In three-terminal structure, the bottom of each sub-cell is electrically connected to the top of the cell. This configuration requires the existence of an intermediate terminal that is difficult to be inserted into its place. Two-terminal series-connected configurations provide the most number of restrictions for the sub-cells interconnecting. This structure requires that the separate sub-cells are of the same polarity and the sub-cell photocurrent is closely matched, as in series connection

the sub-cell with the smallest photocurrent restricts the current generated by the entire cell. The critical advantage of this configuration is that the using of the high-quality monolithic tunnel-junction sub-cell allows making these stacks as monolithic structure with metallization at the very top and bottom of the stack only.

Manufacturing of the two-terminal, series-connected configuration is simpler. In our work, we investigated the QE of this solar cell type.

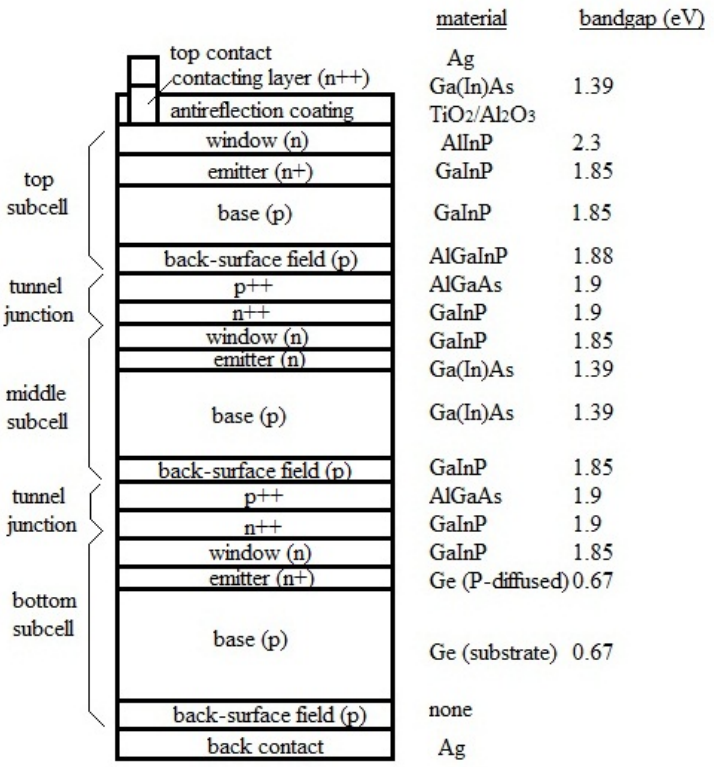


Fig. 18. The structure of a 3J junction GaInP – Ga(In)As – Ge solar cell (Luque, A. & Hegedus, S. 2011). Doping indicated by $n^{++}$, $n^{+}$ and $n$ (or $p^{++}$, $p^{+}$, $p$) corresponds to electron (or hole) concentrations of the order $10^{19} – 10^{20}$, $10^{18}$, $10^{17}$ respectively. Typical materials and their band gaps are indicated. The figure is not on scale.

Two-terminal structure allows absorbing wider spectral range of solar flux that respectively increases the overall conversion efficiency of a solar cell.

It is possible to increase the effieciency of the 3J solar cells by design optimization of each sub-cell. Recently, the efficiency has been improved by using a disordered semiconductor instead of an ordered one, since a disordered one has a higher bandgap.

Moreover, the top sub-cell could be thickened to increase its current production, allowing generating a higher matched current from the whole 3J cell (Yastrebova N.V., 2007).

Another way of enchancement is to add more junctions to the cell. Increasing amount of sub-cells up to five or six allows cutting the solar spectrum into smaller pieces. It makes all subcells better current matched to the low-current producing subcell. Also, this spectrum separation decreases the thermalization losses from electron-hole pairs photogenerated by the photon with energy far above the bandgap. The smaller current density in 5- and 6- junction cell decreases resistive losses.

Theoretical efficiency limits for 1, 2 and 3 junctions are 37, 50 and 56% respectively (Luque, A. & Hegedus, S. 2011). Increasing efficiency when going from one to two or three sub-cells is noticeable, but practically the manufacturing of the solar cells with more than four or five junctions is debatable. Theoretical calculations represent that efficiencies of up to 86.8% can be achieved using an infinite number of sub-cells.

Manufacturing of MJ solar cells is quite expensive in comparison with the amount of electricity they produce, and initially they were used only in space applications. Using concentrators of sunlight makes solar electricity economically justified on the Earth surface. The main part of a photovoltaic concentrator is a low-cost system of lenses or reflectors to focus sunlight on a small area of solar cells. If the concentration aspect is big, then the cost of a solar cell is only a small part of system cost, and in this case the cost of the cell is vindicated.

One of MJ cell manufacturing challenging part is to ensure the transportation between sub-cells. This can be done by implementing a tunnel junction (TJ), which is a stack of highly doped layers, providing an effective potential barrier for both minority charge carriers. This high level of doping is necessary to have a thin depletion region, decreasing optical losses and boosting tunnelling across the junction. Band diagram of the tandem solar cell with the tunnel junction is presented in Fig. 19. It appears between highly $p^{++}$- and $n^{++}$- doped sub-cells layers.

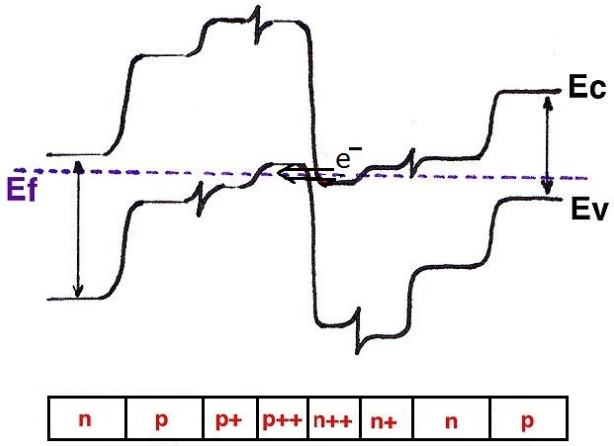


Fig. 19. Band diagram and layers of InGaP – GaAs tandem solar cell with a tunnel junction, modified from (Yamaguchi et al., 2006).

The tunnel-junction between the sub-cells of a multi-junction cell provides a low-resistance connection between a *p*-type back surface field of a sub-cell and a *n*-type window layer of the sub-cell beneath it. Without the TJ, this *p*-*n*-junction has a polarity or forward turn-on voltage that is in opposition to that of the top or bottom cells and, when illuminated, would produce a photo-voltage that could roughly reverse the photo-voltage generated by the top cell (Luque, A. & Hegedus, S. 2011).

### 2.4 Internal and External Quantum Efficiencies

External quantum efficiency (further on denoted as QE) is the ratio of the charge carriers number collected from the solar cell to the number of photons with the certain energy or wavelength (US Department of Energy, 2011). This is one of the most important characteristics of solar cells (and other photodetectors) describing transferring solar flux into electrical energy. QE is a function of either wavelength or photon energy and refers to the response of a solar cell to the various wavelengths.

This efficiency is a correlation between an output and an input. In other words, it is a ratio of electrons produced by the cell to the photons absorbed.

There are two types of QE:

1. QE shows the influence of optical losses in the cell and light reflection from the cell. In other words, QE depends on both the absorption of light and the collection of charge carriers.

2. Internal QE (IQE) is the ratio of the current from the solar cell to the quantity of absorbed photons. IQE describes the ration of photon amount that interacted with the cell (excluding light that has not passed through the cell or was reflected away from it) to the amount of generated charge carriers. QE is calculated from the measured spectral response by taking into account the calibrated response of the reference detector. (Actually, that was done during the measurements of solar cell QE in this work.) IQE is calculated from the QE by taking into account the reflected and transmitted part of the light. IQE describes only the photon amounts converted into charge carriers inside semiconductor. IQE does not include the total amount of generated charge carriers that can be collected at semiconductor contacts.

In our experiments we used the data of the calibrated detectors presented in the units of spectral responsivity *R* (*amperes* per *watt*) as a function from the wavelength. Spectral responsivity is the ration of the current produced by the cell to the light beam power.

In the experimental part of this work, all the quantum efficiencies obtained are external quantum efficiencies. QE of the solar cell as a function from the photon wavelength was calculated using the following equation:

$$QE(\lambda) = \frac{R}{\lambda} \cdot \frac{hc}{e} \cdot \frac{I_{samp}}{I_{ref}} = \frac{R(\lambda)}{\lambda} \cdot \frac{I_{samp}}{I_{ref}} \cdot 1240 \quad , \qquad (10)$$

where $R$ is the calibrated photodetector spectral responsivity, $\lambda$ is a wavelength, $h$ is the Planck constant, $e$ is an elementary electric charge, $I_{\text{samp}}$ is the current generated by a solar cell, and $I_{\text{ref}}$ is the current generated by the reference calibrated detector. According to this formula, QE was measured on a scale from 0 to 1.

# 3 MOUNTING SYSTEM FOR QUANTUM EFFICIENCY MEASUREMENTS

## 3.1 Original system and measurement technique

Present work has been started on the equipment that actually allows carrying out the measurements of single-junction solar cell only. The diagram of the experiment set is shown in Fig. 20.

The original system for 1J solar cells measuring consists of the following elements: halogen lamp *1* is used as a source of light similar to the solar spectrum. The operational spectral range of the beam from the lamp is controlled by filter bank *2* (750 nm short-pass filter, 550 nm high-pass filter, 950 nm short-pass filter, and 800 nm high-pass filter). The filters are chosen according to required wavelength range for a certain solar cell. Further, the beam enters into monochromator Digikom240 (CVI Laser Corporation) with two adjustable gratings. Two manually adjustable apertures *4* are mounted on the exit slit of the monochromator in order to collimate the beam. The monochromatic beam proceeds into the focusing objective *6* through the chopper *5* regulated by controller SR540 (Stanford Research Systems). A solar cell is placed on a 3-axis roller block *7* with differential micrometers. These micrometers provide precise displacement of a sample under focused beam.

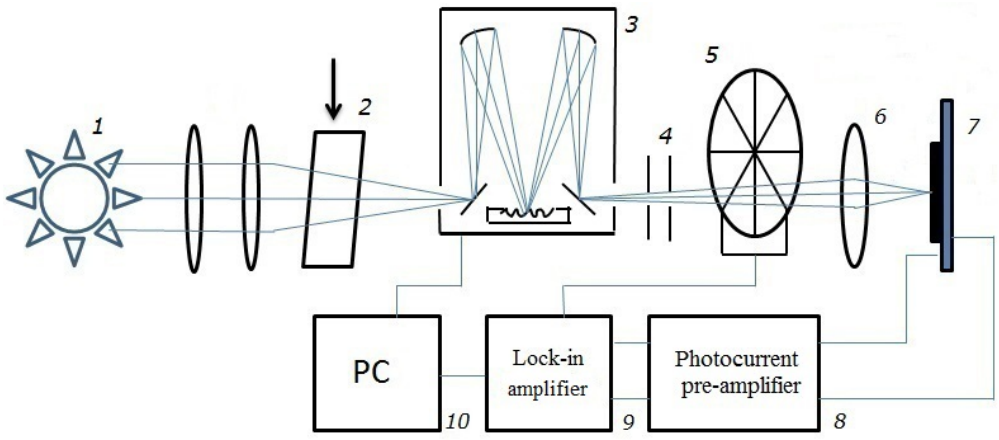


Fig. 20. Diagram of the measuring system: *1* is source of light, *2* is a set of filters, *3* is a monochromator, *4* are adjustable apertures, *5* is a chopper, *6* is a objective lens, *7* is a cell sample on a substrate, *8* is photocurrent pre-amplifier, *9* is lock-in amplifier, *10* is personal computer.

Measured current from a solar cell sample is amplified by photocurrent-voltage amplifier P-9202-4 and afterwards this signal is fed to the lock-in amplifier SR830 (Stanford Research Systems). A personal computer (PC) *10* is controlling the monochromator and is registering the voltage from lock-in amplifier. PC is running LabView software and performs monochromator gratings adjustments.

Lock-in tecnique used in the measurements allows filtering a photocurrent generated by solar cell from a dark diode current in the moments when the cell is covered by chopper wheel (Lu, M. 2008). This current separating happens in a way that only photocurrent as alternating current is registered, and any direct current is discarded (Rand, B. 2014). Photocurrent is magnified and phase-senitively registered by lock-in amplifier. This tecnique allows recording small current signals produced by chopped monochromatic light beam.

### 3.2 Improvements made to the new system

Original system (Fig. 20) was designed only for the measurements of 1J solar cells because it did not have any arrangements for current matching of multi-junction cells. The switching and tuning unit *11* with the set of LEDs *12* were added (in Fig. 21). This system enhancement allows measuring QE of double- and three-junction solar cells type. It would be possible to measure QE of the solar cells with large quantity of junctions by adding LEDs.

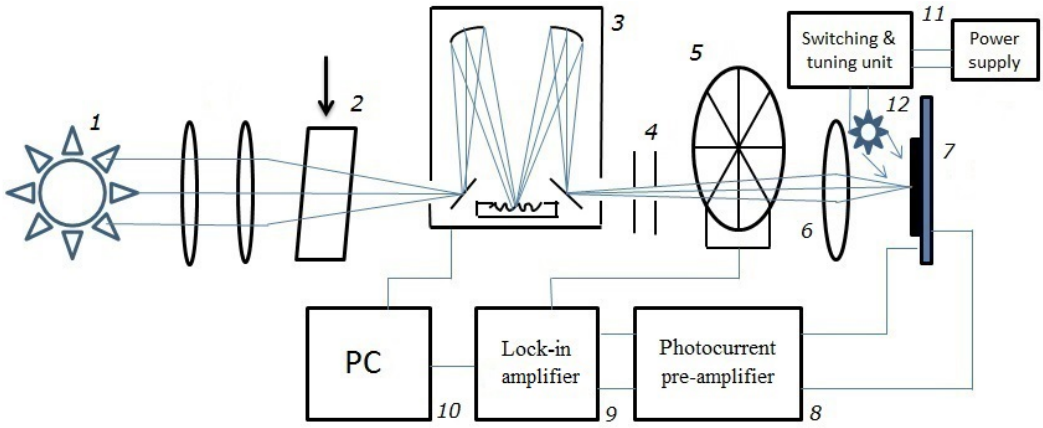


Fig. 21. Improved measuring system for MJ solar cells: *11* is the switching unit with the power supply, *12* is a light bias LEDs.

Two reference detectors that have been calibrated against National Institute of Standards and Technology traceble detector are used for the measurements. The first one is silicon detector FDS100 with known responsivity for 350 to 1000 nm wavelength range. The second detector is germanium detector FDG03 calibrated in the range of 800 to 1600 nm. The responsivity of each detector is used for calculations of QE of the samples using equation (10).

Additionally, it was decided to take into consideration probable influence of stray light from the lamp on a solar cell.

These improvements allow measuring QE of multi-junction solar cells.

### 3.2.1 Light bias

The measurements of QE of 2J and 3J solar cells are carried out as separate and consecutive measurements of single sub-cells connected in series. Since operating sub-cell with minimum current density limits the total current of the double- or triple-junction stack, it is important to match the current densities of each of the cell components at the maximum available point for each sub-cell (Luque, A. & Hegedus, S. 2011).

In the experiment we resolved this current mismatch using blue or IR bias light with certain wavelength for sub-cell saturation.

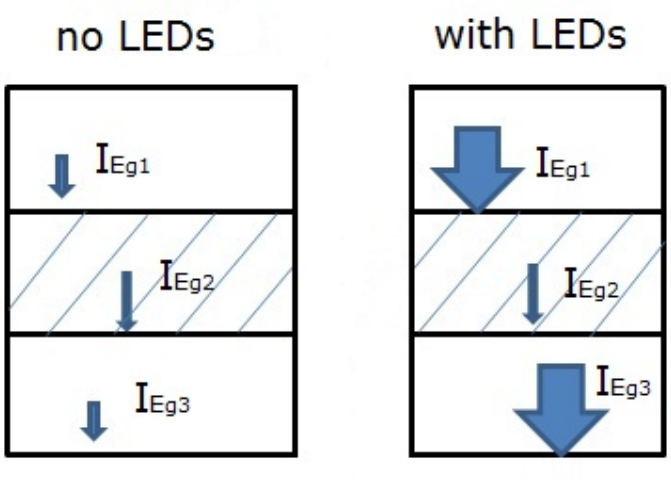


Fig. 22. Schematic view of the sub-cells currents during the measurements with and without LEDs. Wider arrows represent larger sub-cell currents, measured sub-cell is shaded.

The stacked architecture of monolithically grown multi-junction solar cells does not allow measuring each sub-cell current individually because it is technically impossible to attach separate electrodes to each sub-cell. Thus, one of the main goals of the present work was to measure each sub-cell current separately. Serial connection of sub-cells brings the following limitation

$$I_{cell} = \min(I_{E_{g1}}, I_{E_{g2}}, I_{E_{g3}}), \qquad (11)$$

where $I_{Eg1}$, $I_{Eg2}$, $I_{Eg3}$ are the currents from corresponded sub-cells. Total current of the 3J cell equals or is limited by sub-cell minimum current. In other words, the currents through

each sub-cell are retained at one level. Sub-cell current is proportional to the number of incident photons with energy exceeding the semiconductor bandgap and the absorption factor of the semiconductor. Semiconductor absorption factor determines the thickness of a sub-cell. The sub-cell materials should be chosen with desired bandgaps and lattice constants.

As described above, for QE measurements of each sub-cell as the part of 2J or 3J solar cells one needed to separate electrically one sub-cell from another. In order to differentiate the current from one sub-cell, we should keep the currents of two others sub-cells on the maximum achievable level. This could be accomplished by illuminating the solar cell with a LED with certain wavelength related to the sub-cell bandgap (Fig. 22). Photo of LED set is shown in Fig. 23. The characteristics of LEDs used and sub-cell materials of 3J cell are represented in the Table 2.

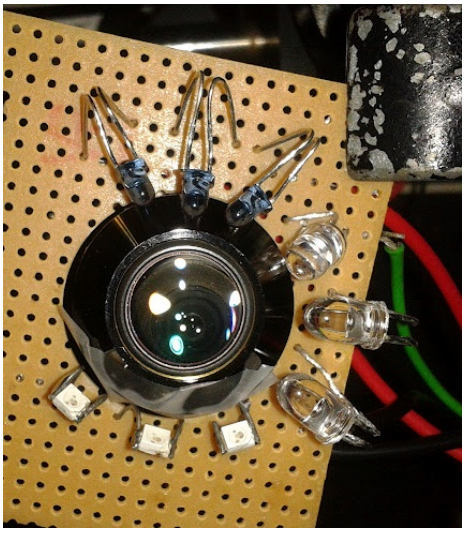

Fig. 23. Set of LEDs that was fixed near the focused beam from the objective.

**Table 2**. Types of LEDs used for sub-cells saturation.

| Sub-cell | Sub-cell material | LED type | Operational wavelength of LED, nm | Wavelength range of QE measurement, nm |
|---|---|---|---|---|
| top | InGaAs | IR | 940 | 800 — 1600 |
| middle | GaAs | IR | 840 | 550 — 950 |
| bottom | InGaP | blue | 440 | 350 — 750 |

During QE measurements, for example, InGaAsN sub-cell, LEDs with working wavelengths 840 nm and 440 nm for saturating GaAs and InGaP sub-cells were used respectively. In other words, certain light bias illuminates and saturates the middle and the bottom sub-cells of the 3J cell. Hence, the current of the top sub-cell is determined by monochromatic beam energy from the halogen lamp only. Top sub-cell current determines 3J solar cell photocurrent. The other two sub-cells are measured in the same way using different kinds of light bias. LEDs with operational wavelengths 440 and 940 nm are used to measure the middle sub-cell and LEDs with wavelengths 440 and 840 nm to measure the bottom sub-cell.

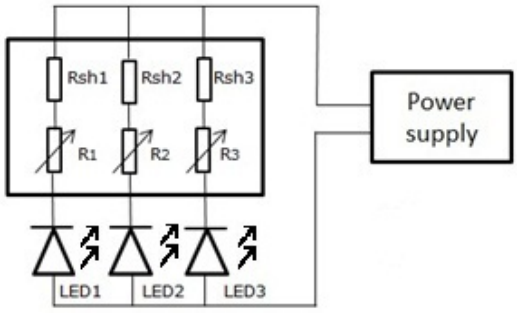


Fig 24. Sub-cell saturation LED schematic. $R_{sh1}$, $R_{sh2}$, $R_{sh3}$ are shunt resistors, $R_1$, $R_2$, $R_3$ are tuning resistors.

The equipment included three samples of each type of LED wired serially to ensure that light intensity of certain wavelength would be sufficient for sub-cell saturation. LED power supply circuit is shown in Fig. 24. Tuning resistors were used for gradually increasing the current through the LEDs up to their maximum supported level.

### 3.2.2 Covering against stray light

In order to achieve the best possible results, all the experiments were carried out in a black-out room with drawn curtains. An overall view of the measuring equipment is shown in Fig. 25. A simple black cardboard cover was used for stray light suppression from the source lamp. To ensure proper cooling, a special ventilation hole *2* in this cover was made. A cooler for the halogen lamp was placed in the hole *2*. Optical filter replacement was performed through a small shutter *3* in the cover.

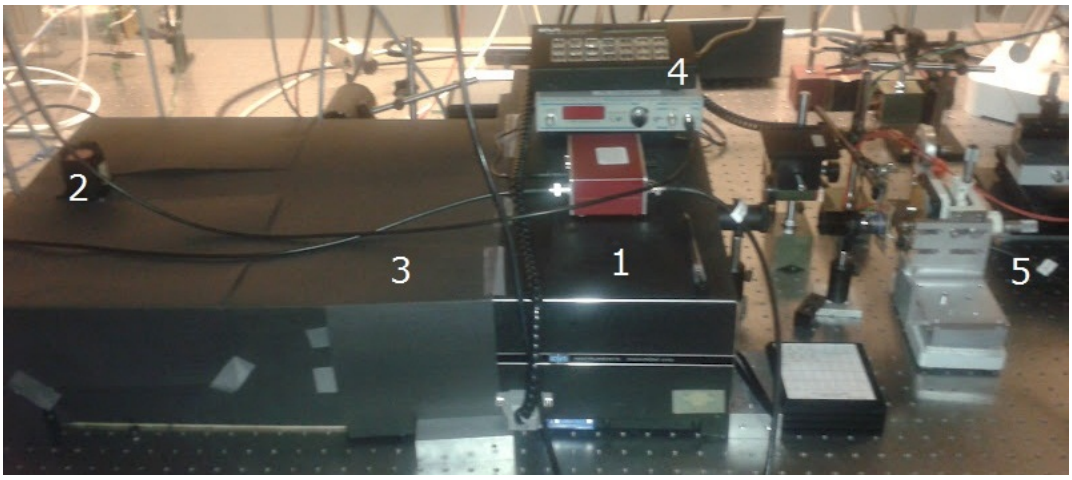


Fig. 25. Overall view of assembled equipment for the measurement of QE.
*1* is the monochromator, *2* is the halogen lamp, *3* is a shutter in cardboard cover, 4 is lock-in amplifier, 5 is a platform with a solar cell.

# 4 RESULTS COLLECTED FROM MODIFIED SYSTEM

In this chapter we present some results that were obtained using measurement system before and after improvement. Enhanced equipment allows measuring the QE of 2J and 3J solar cells. Basically, improved system records current levels generated by a solar cell after exposing under monochromatic light beam. After the measurements, the dependence of QE vs. wavelength was calculated using formula (11). To test the modified system, the QE of 1J cell G0636 and G0639 were measured in the wavelength range from 800 to 1600 nm. The experimental results are shown in Fig. 26. Numbers in brackets (for example, G0636 (11)) mean different pieces of the same sample. As one can observe, G0636 sample QE decreases dramatically at 1400 nm and G0639 sample QE has lower values starting from 800 nm but, in the same time, decreases more gradually and still has some resposivity after 1500 nm.

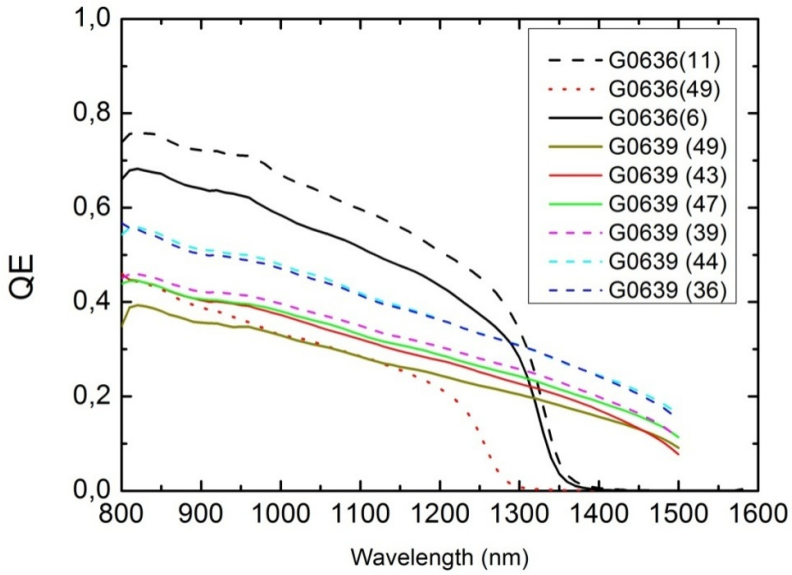


Fig. 26. QE values of G0636 and G0639 1J cell samples.

The QE dependency of annealed and un-annealed (as grown (AG)) 2J solar cells measured on modified system are shown in Fig. 27.

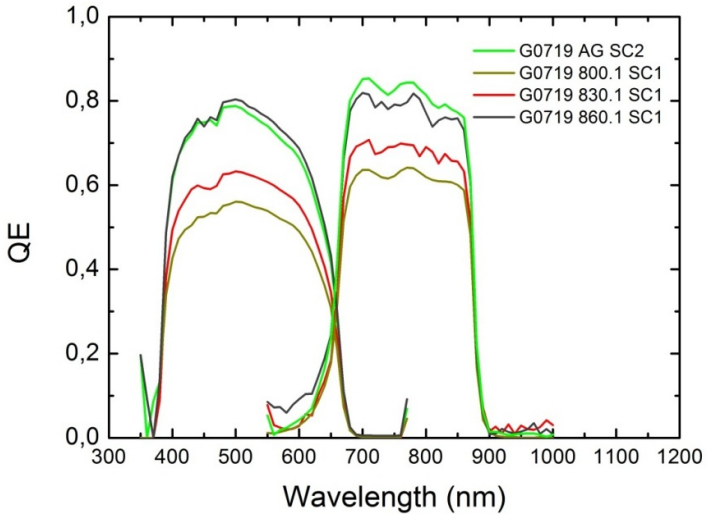


Fig. 27. QE of G0719 2J samples vs. wavelength.

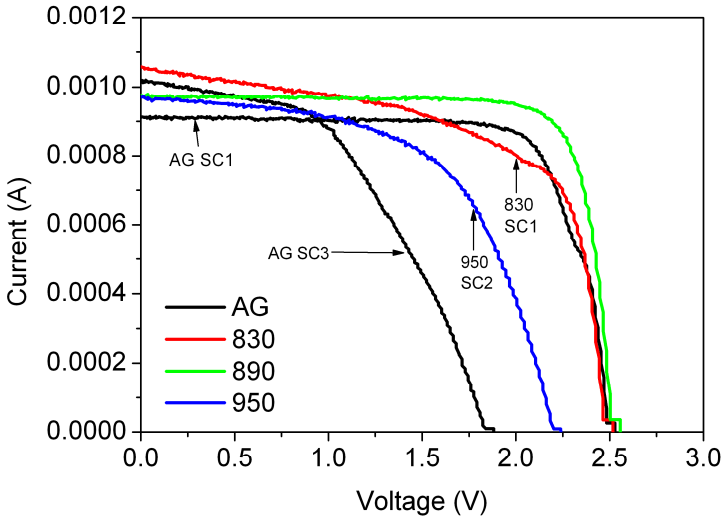


Fig. 28. *I-V* curves for G0719 samples.

The sample quality was estimated according to shape of *I-V* curves obtained at our laboratory and is shown in Fig. 28. According to the graph, the best sample is G0719 890.1 SC1 and hence, the dependence of QE of this sample is shown in Fig. 29.

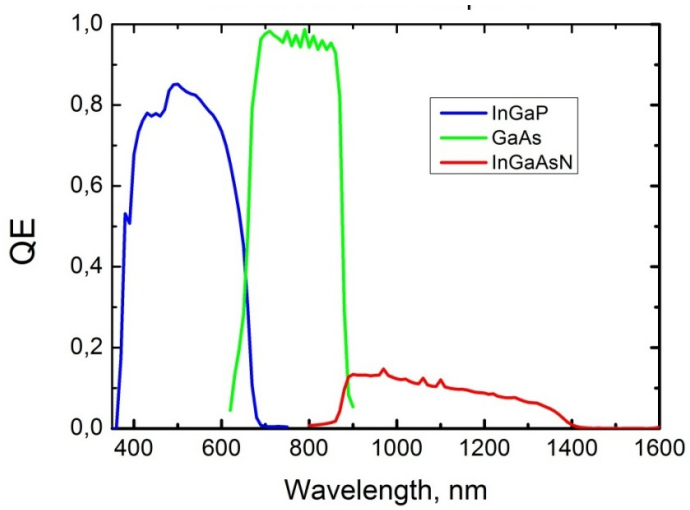


Fig. 29. Calculated QE of 3J solar cell represented as three separated curves.

The maximum QEs for the GaInP cells are in both cases (Fig. 27 and Fig. 29) over 80%. The QEs measured for individual sub-junctions of a GaInP/GaAs/GaInNAs 3J cell were the first ones that were successfully measured at ORC. The low QE measured for the GaInAsN sub-junction is an important result because such knowledge is exactly what one needs to dig out from the MJ solar cells. When one knows which of the sub-junction is producing the lowest current, then it is possible concentrate on improving that junction.

# 5 PERSPECTIVES AND CONCLUSIONS

It was shown that one of the modern tendencies in development of alternative energy source is using of solar energy.

Nowadays using of solar cell modules as basic elements of solar energy systems shows a growing dynamics. This growth is mainly limited by economical feasibility and by cost of the electricity produced by the solar cells. Current perspectives attest that in the next decades this cost will be reduced considerably. Cost reduction boosts the development and makes using of the solar power energy wider.

In this thesis the basic structure, operational principals and main properties of single- and multi-junction solar cells are considered and discussed.

It was declared that the conversion efficiency of 1J solar cells is restricted in accordance with the Shockley-Queisser limit. Using of MJ cells is the way to considerably increase the QE in a wide wavelength range. For experimental investigations of multi-junction solar cells the existing system in our laboratory was modified. This equipment allows carrying out measurements of conversion efficiency of 1J and MJ solar cells using improved disposition of light bias diodes with easy tuning of their currents that effect on the level of sub-cells saturation. Additionally, was developed a principal scheme of the convenient switcher, that allows switching the LEDs and connecting them with the current source without physical replacement of the voltage cables.

The QE as a function of wavelength for 1J and MJ solar cells manufactured at our laboratory were measured using modified system.

In the nearest future, this installation will be used for the demanding QE measurements of MJ solar cells producing by ORC laboratory.

**REFERENCES**

Afanasiev, V. et al. 2011. Silicon thin-film solar elements. Saint-Petersburg, SPbGETU "LETI"

Bishop, R. 2002. The Mechatronics Handbook. CRC Press, p. 19-125.

Burnett, B. 2002. The basic physics and design of III-V multijunction solar cells, [online document]. [Accessed 04 March 2015]. Available at http://www.uotechnology.edu.iq/eretc/books/NRELokok.pdf

Honsberg, Ch. et al. 2010. Photovoltaic Education Network, UNSW [online document]. [Accessed 14 April 2012]. Available at http://pveducation.org/pvcdrom

Kaltschmitt, K. et. al. 2007. Renewable Energy: Technology, Economics and Environment. Springer Science & Business Media, p. 237.

Lorenzo, E. et al. 1994. Solar Electricity: Engineering of Photovoltaic Systems. Sevilla, Progensa.

Lu, M. 2008. Silicon Heterojunction Solar Cell and Crystallization of Amorphous Silicon. USA: UMI Microform, p. 53.

Luque, A. & Hegedus, S. 2011. Handbook of Photovoltaic Science and Engineering. 2nd ed. England: John Wiley & Sons, pp. 111-112, 349, 361, 365, 524-525.

Markvart, T. 1994. Solar Electricity. England: John Wiley & Sons.

National Renewable Energy Laboratory website. 2015 [online document]. [Accessed 16 February 2015]. Available at http://www.nrel.gov/ncpv/images/efficiency_chart.jpg

Stallinga, P. 2009 Electrical Characterization of Organic Electronic Materials and Devices. Wiley. [online document] [Accessed 17 February 2015]. Available at http://www.stallinga.org/ElectricalCharacterization/2terminal/index.html

Philipps, S. et al. 2014. Photovoltaics Report. Fraunhofer ISE, p. 24.

Rand, B. 2014. Organic Solar Cells: Fundamentals, Devices, and Upscaling. CRC Press, p. 452.

Schroder, D. 2006. Semiconductor Material and Device Characterization. Wiley-IEEE Press, p. 404.

Schubert, E.F., 2006. Light Emitting Diodes [online document] [Accessed 18 April 2012]. Available at http://www.ecse.rpi.edu/~schubert/Light-Emitting-Diodes-dot-org/chap12/chap12.htm

Shockley, W. & Queisser, H. 1961. Detailed Balance Limit of Efficiency of p-n Junction Solar Cells. *Journal of Applied Physics*, vol. 32, pp. 510 – 519.

U.S. Department of Energy, 2011. Photovoltaic Cell Quantum Efficiency [online document]. [Accessed 26 April 2012]. Available at http://www.eere.energy.gov/basics/renewable_energy/pv_cell_quantum_efficiency.html

Yamaguchi et al., 2006. *Solar Energy Materials & Solar Cells*, vol. 90, pp. 3068 – 3077

Yastrebova N.V., 2007. High-efficiency multi-junction solar cells: current status and future potential. [online document]. [Accessed 22 February 2015]. Available at http://sunlab.eecs.uottawa.ca/wp-content/uploads/2014/pdf/HiEfficMjSc-CurrStatusFuturePotential.pdf

Young M., 1977. Optics and Lasers: An Engineering Physics Approach. Berlin Springler-Verlag Heidelberg.